Liquid crystal Adaptive Optics Visual Simulator: Application to testing and design of ophthalmic optical elements

Silvestre Manzanera, Pedro M. Prieto*, Diego B. Ayala, Joseph M. Lindacher†, and Pablo Artal

Laboratorio de Optica, Universidad de Murcia (LOUM), Centro de Investigación en Óptica y Nanofísica (CiOyN)
Edificio CiOyN, Campus de Espinardo, E-30071 Murcia (Spain)
†CIBA Vision, Duluth, GA 30097 USA
*****Corresponding author: pegrito@um.es*

http://lo.um.es

Abstract: The concept of Adaptive Optics Visual Simulation applies to the use of an Adaptive Optics system to manipulate ocular aberrations in order to perform visual testing through a modified optics. It can be of interest both to study the visual system and to design new ophthalmic optical elements. In this work, we describe an apparatus based on a liquid crystal programmable phase modulator and explore its capabilities as a tool in the early stages of the design of ophthalmic optical elements with increased depth of field for presbyopic subjects. To illustrate the potential of the instrument, we analyze the performance of two phase profiles obtained by a hybrid optimization procedure. The liquid crystal Adaptive Optics Visual Simulator can be used to experimentally record the point spread function for different vergences in order to objectively measure depth of focus, to perform different psychophysical experiments through the phase profile in order to measure its impact on visual performance, and to study the interaction with the eye's particular aberrations. This approach could save several steps in current procedures of ophthalmic optical design and eventually lead to improved solutions.

OCIS codes: (999.9999) Visual simulation; (330.5370) Physiological optics; (330.4460) Ophthalmic optics; (010.1080) Adaptive optics; (230.6120) Spatial light modulators; (230.3720) Liquid-crystal devices; (330.5510) Psychophysics

References and Links

1. A. W. Dreher, J. F. Bille, R. N. Weinreb, "Active optical depth resolution improvement of the laser tomographic scanner," Appl. Opt. **28**, 804-808 (1989).
2. P. Artal, R. Navarro, "High-resolution imaging of the living human fovea: measurement of the intercenter cone distance by speckle interferometry," Opt. Lett. **14**, 1098-1100 (1989).
3. Liang J., Williams D. R., Miller D. T., "Supernormal vision and high-resolution retinal imaging through adaptive optics," J. Opt. Soc. Am. A **14**, 2884-2892 (1997).
4. F. Vargas-Martín, P. M. Prieto, P. Artal, "Correction of the aberrations in the human eye with a liquid-crystal spatial light modulator: limits to performance," J. Opt. Soc. Am. A **15**, 2552-2562 (1998).
5. E. J. Fernández, I. Iglesias, P. Artal, "Closed-loop adaptive optics in the human eye," Opt. Lett. **26**, 746-748 (2001).
6. H. Hofer, L. Chen, G. Y. Yoon, B. Singer, Y. Yamauchi, D. R. Williams, "Improvement in retinal image quality with dynamic correction of the eye's aberrations," Opt. Express **8**, 631-643 (2001), http://www.opticsinfobase.org/abstract.cfm?URI=oe-8-11-631.
7. P. J. W. Hands, S. A. Tatarkova, A. K. Kirby, G. D. Love, "Modal liquid crystal devices in optical tweezing: 3D control and oscillating potential wells," Opt. Express **14**, 4525-4537 (2006), http://www.opticsinfobase.org/abstract.cfm?URI=oe-14-10-4525.
8. T. R. M. Sales, G. M. Morris, "Axial superresolution with phase-only pupil filters," Opt. Commun. **156**, 227-230 (1998).

#87831 - $15.00 USD Received 24 Sep 2007; revised 15 Nov 2007; accepted 19 Nov 2007; published 21 Nov 2007

9. M. Martinez-Corral, M. T. Caballero, E. H. K. Stelzer, J. Swoger, "Tailoring the axial shape of the point spread function using the Toraldo concept," Opt. Express **10**, 98-103 (2002), http://www.opticsexpress.org/abstract.cfm?URI=oe-10-1-98.
10. M. P. Cagigal, J. E. Oti, V. F. Canales, P. J. Valle, "Analytical design of superresolving phase filters," Opt. Commun. **241**, 249-253 (2004).
11. E. J. Fernandez, S. Manzanera, P. Piers, P. Artal, "Adaptive optics visual simulator," J. Refrac. Surg. **18**, S634-S638 (2002).
12. P. Artal, L. Chen, E. J. Fernandez, B. Singer, S. Manzanera, D. R. Williams, "Neural compensation for the eye's optical aberrations," J. Vision **4**, 281-287 (2004), http://journalofvision.org/4/4/4/.
13. P. A. Piers, E. J. Fernández, S. Manzanera, S. Norrby, P. Artal, "Adaptive optics simulation of intraocular lenses with modified spherical aberration," Invest. Ophthalmol. Vis. Sci. **45**, 4601-4610 (2004)
14. P. A. Piers, S. Manzanera, P. M. Prieto, N. Gorceix, P. Artal, "The use of adaptive optics to determine the optimal ocular spherical aberration," J. Cataract Refr. Sur. **33**, 1721-1726 (2007).
15. L. Lundström, S. Manzanera, P. M. Prieto, D. B. Ayala, N. Gorceix, J. Gustafsson, P. Unsbo, P. Artal, "Effect of optical correction and remaining aberrations on peripheral resolution acuity in the human eye," Opt. Express **15**, 12654-12661 (2007), http://www.opticsinfobase.org/abstract.cfm?URI=oe-15-20-12654.
16. P. M. Prieto, E. J. Fernandez, S. Manzanera, P. Artal, "Adaptive optics with a programmable phase modulator: applications in the human eye," Opt. Express **12**, 4059-4071 (2004), http://www.opticsexpress.org/abstract.cfm?URI=oe-12-17-4059.
17. E. J. Fernandez, B. Povazay, B. Hermann, A. Unterhuber, H. Sattmann, P. M. Prieto, R. Leitgeb, P. Ahnelt, P. Artal, W. Drexler, "Three-dimensional adaptive optics ultrahigh-resolution optical coherence tomography using a liquid crystal spatial light modulator," Vision Res. **45**, 3432-3444 (2005).
18. P. M. Prieto, F. Vargas-Martin, J. S. McLellan, S. A. Burns, "Effect of the polarization on ocular wave aberration measurements," J. Opt. Soc. Am. A **19**, 809-814 (2002).
19. D. Miller, L. Thibos, X. Hong, "Requirements for segmented correctors for diffraction-limited performance in the human eye," Opt. Express **13**, 275-289 (2005), http://www. opticsexpress.org/abstract.cfm?URI=oe-13-1-275.
20. P. M. Prieto, F. Vargas-Martin, S. Goelz, P. Artal, "Analysis of the performance of the Hartmann-Shack sensor in the human eye," J. Opt. Soc. Am. A **17**, 1388-1398 (2000).
21. A. B. Djurisic, J. M. Elazar, A. D. Rakic, "Simulated-annealing-based genetic algorithm for modeling the optical constants of solids," Appl. Opt. **36**, 7097-7103 (1997).
22. G. Zhou, Y. Chen, Z. Wang, H. Song, "Genetic local search algorithm for optimization design of diffractive optical elements," Appl. Opt. **38**, 4281-4290 (1999).
23. D. Marquardt, "An algorithm for least-squares estimation of nonlinear parameters," J. Soc. Ind. Appl. Math. **11**, 431-441 (1963).
24. L. Llorente, L. Diaz-Santana, D. Lara-Saucedo, S. Marcos, "Aberrations of the human eye in visible and near infrared illumination," Optom. Vision Sci. **80**, 26-35 (2003).
25. E. J. Fernandez, A. Unterhuber, P. M. Prieto, B. Hermann, W. Drexler, P. Artal, "Ocular aberrations as a function of wavelength in the near infrared measured with a femtosecond laser," Opt. Express **13**, 400-409 (2005), http://www.opticsexpress.org/abstract.cfm?URI=oe-13-2-400.

1. Introduction

Adaptive Optics (AO) was initially developed in the Military and Astronomy fields, to actively manipulate the wavefront of an optical system in order to compensate the aberrations and, consequently, improve its performance. Among the initially proposed applications of the technology were high-power laser focusing, free-space communications and high resolution imaging through turbulent media. Visual Optics is another field where considerable effort has been made to apply AO techniques since the early 90's, when a segmented mirror [1] and speckle interferometry [2] were applied to the eye. More recently, static corrections of ocular aberrations and real-time closed-loop AO were demonstrated [3-6]. In these cases, the typical uses include improved vision and high resolution retinal imaging. All the above mentioned applications are based on the cancellation of aberrations, to produce a nearly-perfect system from an optical point of view. However, the ability to manipulate the wavefront opens the possibility to more general applications. For example, AO elements and methods have been used to produce customized point spread function (PSF) shapes for optical micromanipulation [7], and could be exploited to implement super-resolution imaging techniques [8-10].

Visual Simulation is an application of non-zero aberration AO in Vision research. In this case, the ocular wavefront is manipulated with an Adaptive Optics Visual Simulator (AOVS) and visual tasks are performed through modified optics [11]. One use of this technology is the study of higher level functions of the visual system. Artal et al. [12] studied adaptation of the

#87831 - $15.00 USD Received 24 Sep 2007; revised 15 Nov 2007; accepted 19 Nov 2007; published 21 Nov 2007

visual system to the eye's aberrations: A group of subjects carried out visual tasks through an AO system that rotated the ocular aberrations and the results were compared to those for the unmodified eye. The authors found that visual performance was best for the true orientation of the ocular aberrations, suggesting some neural adaptation to the eye's aberrations.

Another application of Visual Simulation is the development of new ophthalmic optical elements. A simplified scheme of the steps currently required for this task is shown in Fig. 1 (left panel). After defining the problem to be tackled, the designer produces a mathematical representation for the phase profile which is implemented in prototypes that can be tested in clinical trials. In case of satisfactory results, the ophthalmic optical design is acceptable. However, if the behavior does not meet the expectations, the design should be discarded or redesigned. The whole procedure can take months to be completed and is costly. The right panel of Fig. 1 sketches the potential benefits of the use of an AOVS for preliminary testing of new phase profile designs. This testing can be performed in a limited number of subjects in minutes or hours. Consequently, the number of designs that can be tried is considerably increased and there is room for more innovative ideas. Furthermore, the outcome of the AOVS testing can be useful to improve the designs, constituting a sort of design loop (red arrows in the right panel of Fig. 1). The best phase profiles generated with this procedure can then be implemented as prototypes, which in turn can be tested on real subjects with the AOVS working in passive mode. This testing can be useful to detect potential failures in the manufacturing or in the adaptation of the ophthalmic optical design (blue arrows). This double filtering of new designs before extensive clinical trials should minimize the risk of a failure at this stage of the process (represented by the dotted arrow) with the corresponding benefit in terms of time and costs. It is also worth mentioning that the use of the AOVS is non-invasive. This property adds an additional advantage when the phase profiles are designed to be implemented in permanent elements, as intra-ocular lenses or refractive surgery profiles.

A different application of Visual Simulation, somehow related to the previous one, is the presentation to a prospective patient of the potential benefits that could be achieved with an advanced wavefront manipulation treatment. The relevance of this kind of pre-treatment test can be small when removable elements (i.e., ophthalmic or contact lenses) are involved. However, it can play a key role in the patient's decision when a non-reversible treatment is intended, as it is the case for customized refractive surgery.

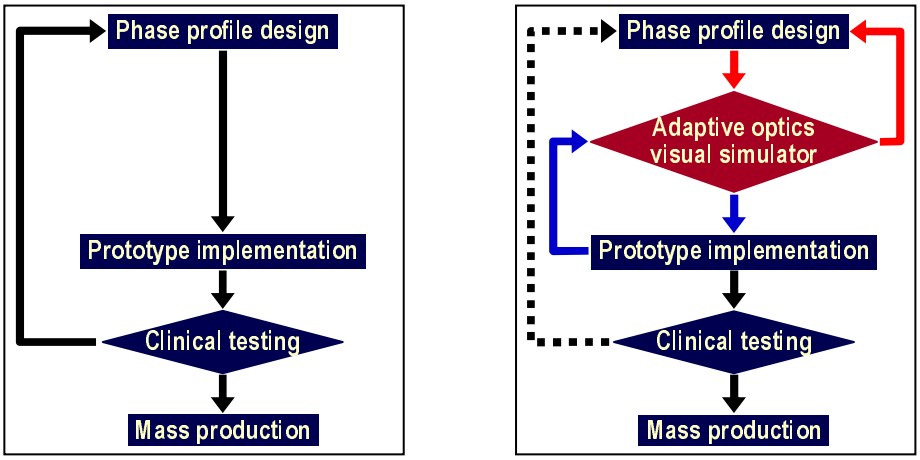

Fig. 1. Simplified scheme of the design procedure for new ophthalmic optics. Left: The current typical design loop requires days or months to be completed. Right: The AOVS allows the implementation of a design loop (red arrows) where a new idea can be tested or improved within minutes or hours. Additionally, it can be used to check the performance of eventual prototypes, supplying information about the manufacturing procedures (blue arrows).

#87831 - $15.00 USD Received 24 Sep 2007; revised 15 Nov 2007; accepted 19 Nov 2007; published 21 Nov 2007

In our laboratory in Murcia, we have extensive experience in the development of AO Visual Simulators. Our first prototype [11] was based on a low-cost membrane deformable mirror (OKO Tech, 37 actuators) and was used both to make initial tests on neural adaptation and as a tool for the development of new aspheric IOLs [13]. More recently, we have upgraded this system with a Xinetics deformable mirror with 97 actuators, and we have tested the amount of spherical aberration that optimizes contrast sensitivity [14]. A similar apparatus has been used to study the effect of modified optics in peripheral acuity [15].

In this work we present an AOVS which has a liquid crystal programmable phase modulator (PPM) as active element for wavefront manipulation. This device is a commercially-available optically-addressed spatial light modulator (Hamamatsu X-8267), which has been already demonstrated for correction of ocular aberrations [16,17]. Compared to deformable mirrors, the PPM is an easy-to-use device with high spatial resolution and no continuity constraints, which allows the generation of very steep phase profiles and the increase of the effective stroke by means of a wrapped phase representation. Additionally, its high linearity and fidelity permits phase generation in a single step or even in open loop. Among its drawbacks are the limited temporal bandwidth, which is not critical for static phase manipulation; the requirement of polarized light, which has been proven to have no impact on wavefront estimation [18]; and the chromatic dispersion, which is not a relevant issue when monochromatic or limited spectral bandwidth light is used [19].

The liquid crystal AOVS (LC-AOVS) has been developed as a tool for the design of advanced ophthalmic optical elements. In particular and as an example, we show in this work the capabilities of the LC-AOVS in the development of multifocal phase profiles that could be implemented in contact lenses. The profiles tested in this case have been obtained by means of a custom-made optimization algorithm. Results are presented for two different multifocal designs. The LC-AOVS can be used to test whether a new model meets the design specifications. This is the case for one of the tested profiles while discrepancies between the visual simulation results and the theoretical expectations are observed for the other. Therefore, the chosen designs illustrate two possible outcomes of Visual Simulation testing: while one of them is validated and can be considered a good candidate for further stages of the process, the other is a partial failure. In this particular case, further testing with the LC-AOVS suggests that the reason for the anomalous behavior of the phase profile is the interaction with the subject's individual aberrations. This kind of design loop, where a newly designed phase profile can be tested within minutes or hours with the LC-AOVS, can be a powerful tool in the development of new ophthalmic optical elements, reducing costs, saving steps, and eventually leading to better solutions.

2. Methods

2.1. Experimental Apparatus

The liquid crystal adaptive optics visual simulator (LC-AOVS) is based on a previously reported AO system [16]. The wavefront sensing is performed by means of a custom-made Hartmann-Shack (HS) sensor [20] and the active element is a liquid crystal programmable phase modulator (PPM) (Hamamatsu X-8267). Figures 2 to 4 show schematic views of the system in its different operating configurations.

There are two illumination channels: one with a spatially filtered, collimated He-Ne laser (633 nm) as light source, which is introduced in the system by reflection in beam splitter BS without going into the eye; the other uses an IR diode laser (780 nm) to illuminate the subject's eye. The IR channel (see Fig. 2) is switched on when the subject's aberrations are to be measured or corrected in close-loop, while the red channel (see Fig. 3) is used for alignment purposes and for testing the stand-alone characteristics of the phase profiles.

The measurement channel contains the PPM and a linear polarizer aligned with the liquid crystal molecules preferred orientation. Also, a Badal system composed of two lenses, two static mirrors, and two sliding mirrors is included. This element is typically used to correct the eye's defocus but in our case it is also useful to check the behavior of the tested profiles for

#87831 - $15.00 USD Received 24 Sep 2007; revised 15 Nov 2007; accepted 19 Nov 2007; published 21 Nov 2007

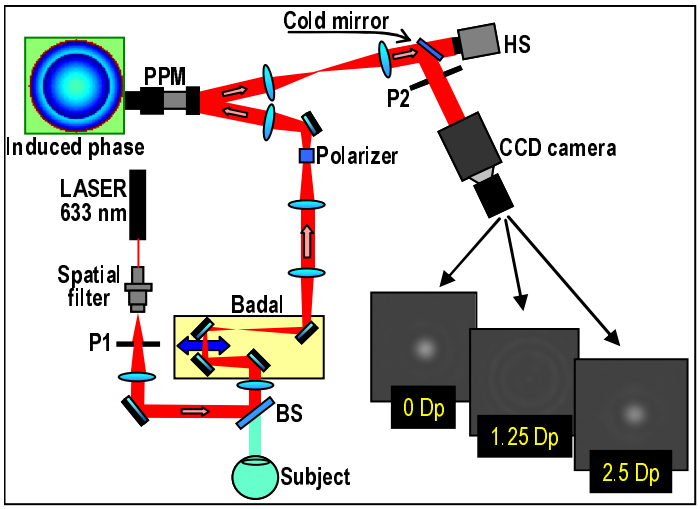

Fig. 2. Schematic view of the 633-nm illumination channel of the LC-AOVS used for alignment and calibration, and for experimental PSF recording. BS: Beam splitter; P1 and P2: Pupils. In light blue the elements not used in this configuration.

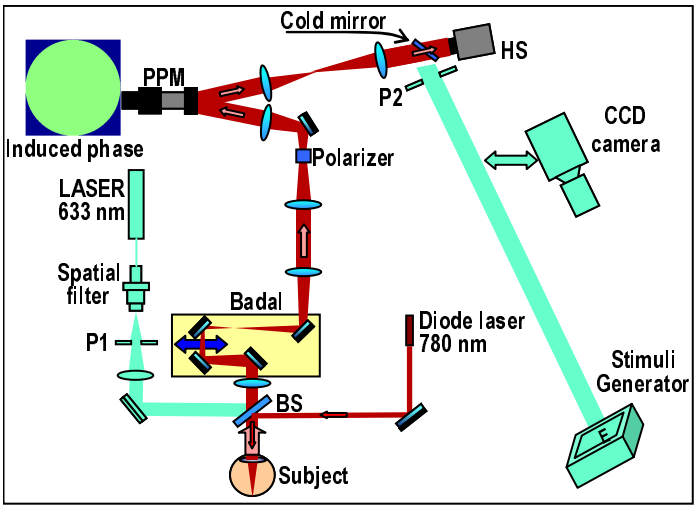

Fig. 3. Schematic view of the IR channel of the LC-AOVS used for ocular aberration measurement and correction. In light blue the elements not used in this configuration.

different focus positions, both objectively, by PSF measurements, and subjectively, using psychophysics experiments. After reflection in the PPM, the light in the measurement channel can be used for aberration measurement with the HS sensor and/or for PSF recording with a CCD camera. The switching between these two different operation modes is done by means of a cold mirror that is basically transparent for IR but reflects a large fraction of red light. Therefore, the He-Ne laser can be used both to record the experimental PSF and to check the aberration pattern displayed in the PPM, while the diode laser is used for ocular aberration measurements and for close-loop AO in the eye.

Finally, the visual channel is shown in Fig. 4, which shares most of the elements of the measurement channel, in particular the cold mirror, the PPM and the Badal system. The visual channel is used to present the subject with stimuli displayed in a high quality monitor to perform different visual tasks. These tasks are used to study the performance of the phase

#87831 - $15.00 USD Received 24 Sep 2007; revised 15 Nov 2007; accepted 19 Nov 2007; published 21 Nov 2007

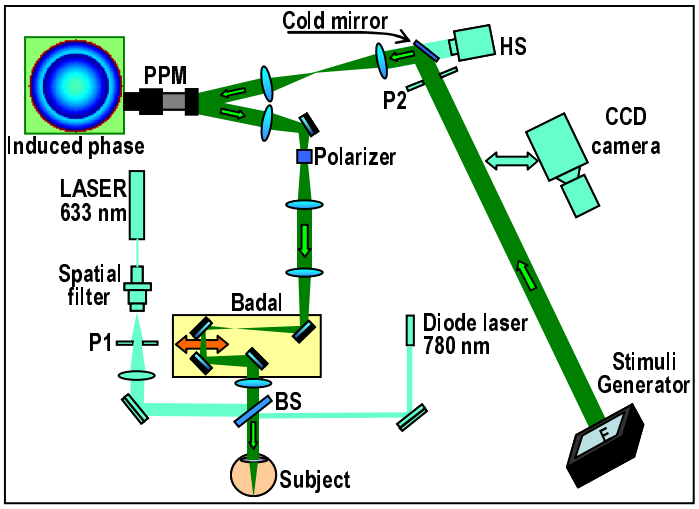

Fig. 4. Schematic view of the visual simulation channel of the LC-AOVS used for psychophysics experiments through a modified ocular optics. In light blue the elements not used in this configuration.

profiles presented in the PPM for different vergences, selected with the Badal system. The visual stimuli are typically presented in green light (using the monitor's green phosphor) and, therefore, they are introduced by reflection in the cold mirror with virtually no loss. Even when the stimuli are presented in white light, the spectral modifications produced by the cold mirror are negligible.

To generate an aberration profile with the PPM, a grey-scaled image containing the wrapped phase map is sent through a computer video port. The software package developed in our lab for controlling the AO system, described in some detail elsewhere [16], is capable of presenting Zernike-based phase profiles or pixel-by-pixel maps. The high fidelity of the PPM for aberration production allows the introduction of a phase profile in a single step. The PPM model X-8267 has an active area of 20×20 mm with XGA resolution (768×768 pixels). The magnification between the subject's pupil plane and the PPM plane is 2.5, which means a maximum pupil size of 8 mm with a resolution of 96 pixels per mm. The calibration procedures to set up the PPM were described in Ref. [16]. They include pupil fine alignment and measurement of the coefficient relating displayed gray level and induced phase, or gain, which depends mainly on the illumination wavelength and therefore has to be separately obtained for each illumination channel.

2.2. Aberration profile testing procedure

The initial step in the aberration profile testing procedure consists of the calculation of the expected image quality associated to the profile considered as an isolated phase plate for a series of conditions. This was performed by calculating the Strehl ratio. The result of this computation can then be compared to the experimental Strehl ratio obtained from the images recorded when the profile is introduced in the PPM and applied to a reference flat wavefront. These steps provide us with information both about the performance of the designed profile and the correct operation of the experimental system. Finally, if the isolated image quality produced by the profile meets the desired specifications, the actual effect on vision can be studied by asking subjects to perform a set of visual tasks through the system with the profile present. The following subsections describe these testing procedures with some detail.

2.2.1. Computation of the theoretical stand-alone image quality

Depending on the procedure used to obtain the aberration profile for a new ophthalmic optical element, the phase map can be represented analytically, e.g., as a Zernike expansion, or pixel

#87831 - $15.00 USD Received 24 Sep 2007; revised 15 Nov 2007; accepted 19 Nov 2007; published 21 Nov 2007

by pixel. In either case, the associated monochromatic PSF is calculated by complex exponentiation and Fourier transform, and the Strehl ratio can be readily obtained from the peak intensity. Since we are interested in the through-focus behavior, we compute the Strehl ratio for each phase map after addition of different amounts of defocus. The results of this through-focus scan can be used as a first estimate of depth of focus for the tested design.

To make the computation closer to actual conditions, the specific aberrations of a subject, which are measured with the apparatus in the configuration shown in Fig. 3, can be added to the phase profile. Typically, this does not produce large effects, which means the ophthalmic optical design is appropriate for a wide population. In some cases, however, differences have been found, particularly when there were also discrepancies with the experimental results. Consequently, this can be a tool in refining the design process. Additionally, the robustness of the profile to lateral displacements, so common in ophthalmic optics, was also estimated by replicating the calculations for different pupil positions.

2.2.2. Determination of the experimental stand-alone image quality

The first experimental checking we carry out consists of recording of the PSF associated to the profile displayed in the PPM. This is performed with the apparatus configuration shown in Fig. 2. The cold mirror sends the beam to the removable CCD camera and the PSF is recorded for a series of vergences, which are set by means of the Badal system. The size of aperture P2 is selected to match the design specifications of the tested profile. From each image obtained, the experimental Strehl ratio is calculated and compared to the theoretical one. It has to be pointed out that this testing is performed in red (633-nm) light while visual testing is carried out in green light. Accordingly, the PPM settings have to be modified between these two tasks to account for the change in wavelength. In particular, the phase map must be converted to optical path and re-wrapped and the appropriate gain has to be used. In analogy to the testing described in the previous section, the experimental Strehl ratio can be obtained for laterally displaced versions of the intended profile.

As an intermediate stage and to check the procedure, we can measure with the HS sensor the aberrations actually introduced by the PPM and then compute the associated PSF. This step makes sense when the designed profile has an analytical form but it is not really useful for pixel-by-pixel profiles because of the limited spatial resolution of the HS.

2.2.3. Visual performance tests

After the objective testing, next step in the evaluation of a given phase profile is the study of its effects on different visual tasks. In order to do this evaluation, the camera for PSF recording is removed to provide the subject with a free path to see a monitor where a collection of visual stimuli can be presented (Fig. 4). The distance from the subject to the monitor is around 3 meters. The size of pupil P2, which is optically conjugate to the subject's pupil, is selected to match the design specifications of the tested profile. The software for stimulus generation makes use of the Cambridge Research System libraries. For the purposes of this work, visual performance was quantified by means of the word recognition acuity, measured by the adjustment method. The target consisted of lower case Spanish words of various lengths presented during 500 ms. Subjects were instructed to vary letter size until they could barely read all the words, typically increasing letter size from a clearly "unreadable" size. Three readings were taken for each experimental condition and the mean and typical deviation were calculated. After one reading, subjects were instructed to largely vary letter size in the two opposite directions before starting the next adjustment series.

In order to test the performance of each phase profile in terms of effective depth of field, the word recognition acuity through the phase profile was measured for a set of vergences. The range spanned from subjective best focus for the naked eye to 3D or 3.5D, depending on the subject, in 0.5D steps. The naked eye's best focus search and the vergence adjustment were performed by means of the motorized Badal system. For comparison purposes, word recognition acuity for the null phase (equivalent to the naked eye) was also tested for the same range of vergences.

#87831 - $15.00 USD Received 24 Sep 2007; revised 15 Nov 2007; accepted 19 Nov 2007; published 21 Nov 2007

2.3. Subjects

Results will be presented for two healthy subjects with normal values of high order aberrations: subject PA is a 44 years old myope (1.5 D), and subject SM is a 32 years old myope (2.75 D). The right eye of each subject was used for testing. Subject SM's accommodation was paralyzed with two drops of tropicamide 1% with thirty minutes interval between them. Conversely, subject PA's eye was not instilled with cycloplegic drops. This subject is already an early presbyope and he was instructed to relax his accommodation and to keep his left eye open throughout the visual testing in order to further reduce his ability to accommodate. Accordingly, while subject SM should respond as a complete presbyope, subject PA would present some residual accommodation.

2.4. Phase profile design: aberration optimization process

To illustrate the capabilities of the LC-AOVS for phase profile testing, we will show results for a series of phase profiles obtained by an optimization procedure, described in this section.

A genetic local search algorithm (GLSA) [21,22] was used to find phase profiles to increase depth of focus. These are hybrid algorithms that combine genetic algorithms (GA) and local search techniques. For this particular implementation of the GLSA, the local algorithm was a Levenberg-Marquardt [23] (LM). Both the genetic and the local methods are designed to maximize the Strehl ratio of the PSF associated to the phase profile for several defocus values. The profile is represented as a phase map with a given pixel resolution. The phase value for each pixel is a fitting parameter, and is pixel-by-pixel modified through both sections of the procedure. Initially the GA is applied, searching for a solution in a wide region of the parameters space. The output is then used as a seed for the LM algorithm, which refines the search. The software developed to implement these algorithms allows us a degree of customization of the through-focus behavior and a selection of the number of points and positions of the secondary foci where the Strehl ratio is maximized. Moreover, it is possible to take into account some features that can occur in real eyes as, e.g., the change in pupil size with vergence or the possibility of residual accommodation in younger presbyopic subjects.

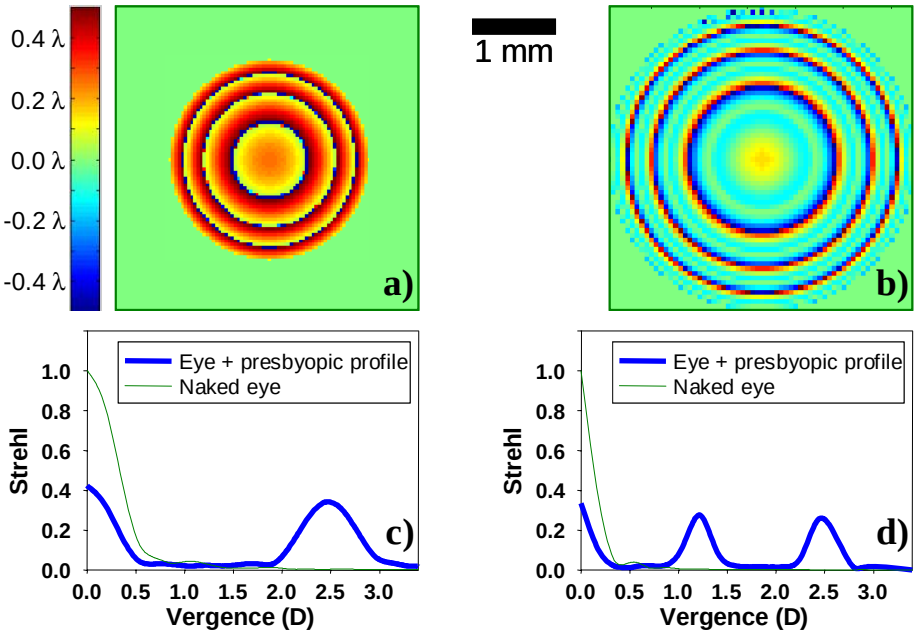

Fig. 5. Multifocal profiles obtained by the hybrid optimization method. Panel (a): bifocal profile over a 2.4-mm pupil. Panel (b): trifocal profile over a 3.6-mm pupil. Panels (c) and (d): theoretical Strehl ratio for each profile (thick blue line) and for the naked eye (thin green line).

#87831 - $15.00 USD Received 24 Sep 2007; revised 15 Nov 2007; accepted 19 Nov 2007; published 21 Nov 2007

Figure 5 shows two examples of phase maps obtained with the GLSA procedure. Figure 5(a) shows the GLSA outcome when a 2.4-mm pupil diameter is considered and the Strehl ratio is optimized for 0D and 2.5D, which corresponds to a bifocal profile. Figure 5(b) shows an example of trifocal profile obtained by optimizing the Strehl ratio for 0D, 1.25D and 2.5D for a 3.6-mm pupil diameter. In both cases, no residual accommodation was considered, i.e., the phase profiles are designed for complete presbyopes. Panels (c) and (d) in Fig. 5 show the theoretically computed Strehl ratio as a function of the defocus for the profiles in panels 5(a) and 5(b) respectively. As a result of the optimization procedure, image quality is clearly improved for defocus values corresponding to the primary and secondary foci of each profile. For comparison purposes, the Strehl ratio as a function of defocus for an aberration-free eye with the selected pupil diameter is plotted as a thinner line.

3. Results

In order to illustrate the operational capabilities of the LC-AOVS, we show the results for the phase maps shown in Fig. 5. These two profiles have been selected because they can exemplify the possible outcome of visual simulation testing: the bifocal profile in Fig. 5(a) shows a behavior in accordance with the design specifications while the trifocal profile in Fig. 5(b) does not respond exactly as expected. Therefore, while the former is a good candidate to be implemented in actual prototypes, the latter could be discarded or redesigned.

Figure 6 shows the results for objective depth of focus analysis. For each phase profile, the thick solid line corresponds to the theoretically computed Strehl ratio as a function of vergence. The yellow solid circles are the experimental Strehl values obtained from the PSFs recorded with the CCD camera for a series of vergences ranging for 0 to 3D in 0.175D steps. The agreement between computed and experimentally obtained Strehl ratio values is quite good. This fact validates both the computation process, which in the case presented here is key for the profile design procedure (based on the optimization of the Strehl for a series of vergences), and also the experimental apparatus. As a further example, Fig. 7 shows examples of the experimental PSFs obtained for different vergences. The secondary foci provided by the presbyopic profiles become readily apparent, as the corresponding PSFs are very similar, both in height and extension, to the PSF for 0D. Conversely, the PSFs for intermediate vergences spread over a much larger area, meaning a reduction on the corresponding image quality.

Once the phase profile behavior has been objectively assessed, its impact on visual performance can be tested. Figure 8 shows results of word recognition acuity as a function of vergence with the bifocal phase profile in Fig. 5(a). The effect is readily apparent when the curves are compared to those obtained for the naked eye, i.e., when a flat phase map is displayed in the PPM: acuity initially declines but peaks again around 2.5D of vergence. This behavior is in good agreement with the expectations, since this phase profile has been designed to optimize Strehl ratio for 0 and 2.5D.

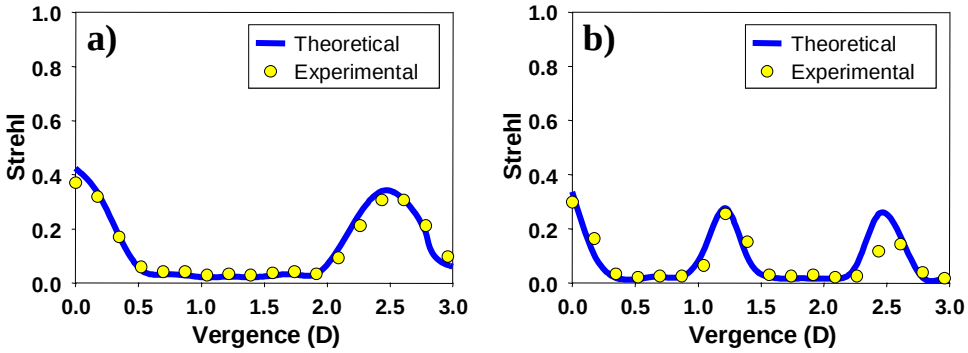

Fig. 6. Experimental Strehl ratio (symbols) obtained from the recorded PSF images and theoretical calculations (lines) for the profiles in Figs. 5(a) (left panel) and 5(b) (right panel).

#87831 - $15.00 USD Received 24 Sep 2007; revised 15 Nov 2007; accepted 19 Nov 2007; published 21 Nov 2007

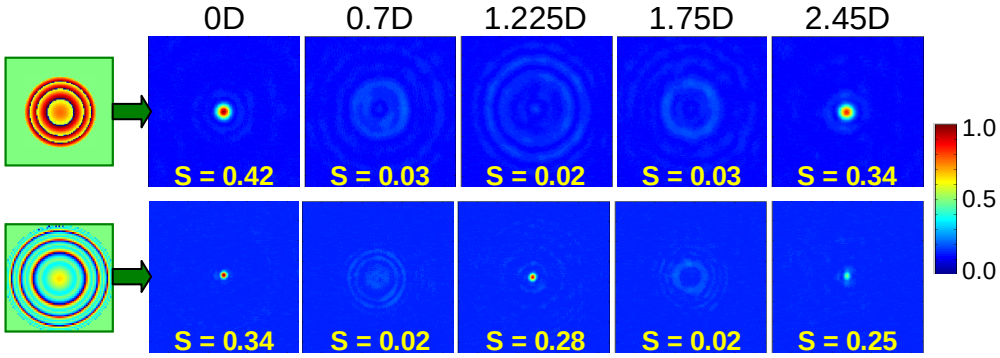

Fig. 7. Examples of PSFs experimentally recorded for the bifocal (upper row) and trifocal (lower row) phase profiles. All images have been rescaled to the maximum intensity of the series. The colorbar is in normalized units. On top of each image, the vergence for which each PSF was obtained. In yellow, the Strehl ratio experimentally obtained in each case.

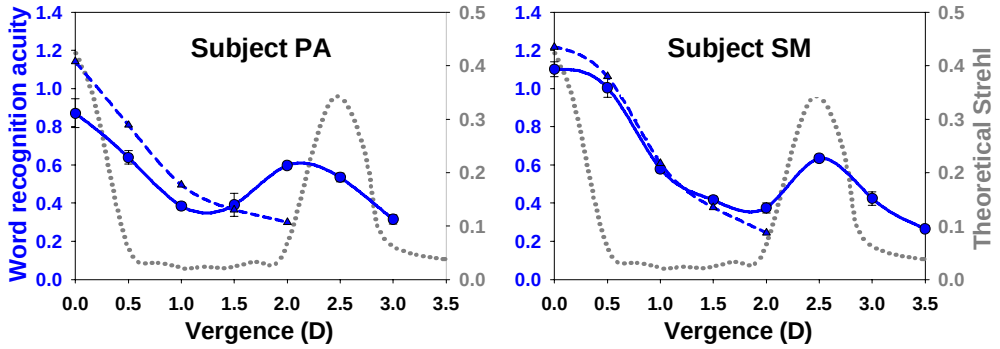

Fig. 8. Plots in blue represent decimal acuity for word recognition for the naked eye (dashed line, triangles) and through the bifocal profile in Fig. 5(a) (solid line, circles). The psychophysical measurements were carried out in 0.5D steps. Error bars (wherever visible) represent standard deviation in three trials. For comparison purposes, we show the theoretical Strehl ratio for this phase profile as a dotted gray line. The scale between the vertical axes has been arbitrarily set to aid visual comparison of the different plots.

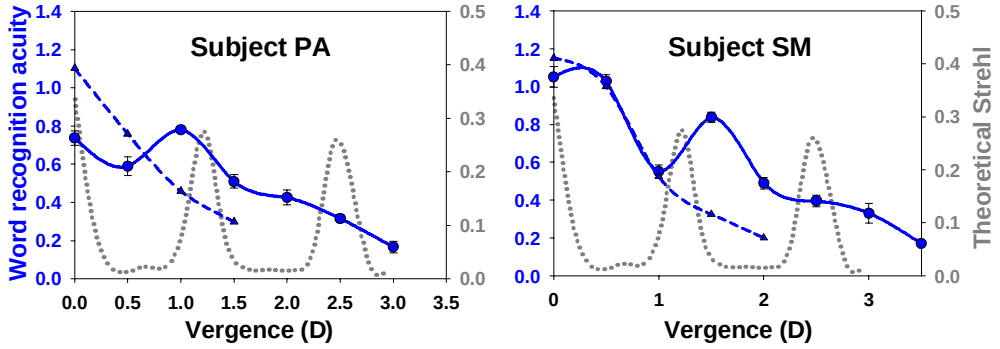

Fig. 9. Decimal visual acuity for word recognition for the naked eye (dashed blue line, triangles), through the trifocal phase profile in Fig 5(b) (solid blue line, circles) and Strhel ratio for this profile (dotted gray line). For more details see caption to Fig. 8.

#87831 - $15.00 USD Received 24 Sep 2007; revised 15 Nov 2007; accepted 19 Nov 2007; published 21 Nov 2007

Figure 9 shows the results of word recognition acuity for the trifocal phase profile shown in Fig. 5(b). The intermediate focus was set at 1.25D by design and the corresponding increase in word recognition acuity can be seen for both subjects. For subject PA the word recognition acuity peaks for 1D while for subject SM the peak appears for 1.5D. The difference between these two values can be due to the 0.5D steps used for the psychophysics testing but it can also be attributed to slight errors in the best focus search for far vision. The behavior of word recognition acuity around 0D suggests that the curve for subject PA is slightly shifted towards smaller vergences and in the opposite direction for subject SM.

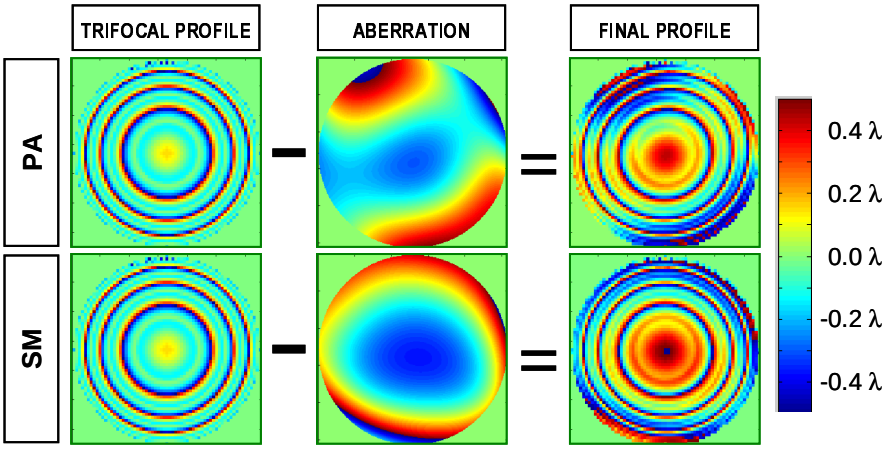

Fig. 10. Customized phase profiles obtained by subtracting the subject's aberrations. In front of the subject's eye should be equivalent to presenting a perfect eye with the profile in Fig. 5(b).

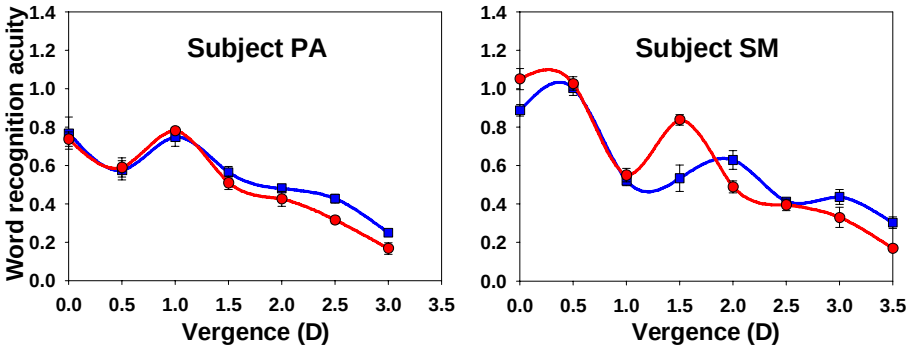

Fig. 11. Comparison between word recognition acuity for the customized trifocal phase profiles in Fig. 10 (blue line, squares) and the phase profile in Fig 5(b) (red line, circles). The latter plots were shown in Fig. 9. Error bars are the standard deviation in the three trials.

Near vision focus was set at 2.5D but neither subject show a peak in acuity around this value. At most, a slight decrease in the decline can be speculated when the curves are compared with those for the naked eye. One potential reason for this departure from the expected behavior could be the interaction between the phase profile and the subject's own aberrations. This point is easy to check with the LC-AOVS, since it allows the measurement of the ocular wavefront. With this information, we can create customized phase maps that compensate the individual's aberrations in order to present the desired profile to the corrected eye. Figure 10 sketches the procedure: for each subject a new phase map is created by subtracting the ocular aberrations from the profile in Fig. 5(b). The addition of this new map to a real eye should be equivalent to presenting the profile to a perfect eye. At this point, it

#87831 - $15.00 USD Received 24 Sep 2007; revised 15 Nov 2007; accepted 19 Nov 2007; published 21 Nov 2007

may be worth noting that the eye's aberrations are measured in IR while the visual tasks are performed in green light. However, it has been found that ocular wavefront barely changes with wavelength in the visible and near infrared [24,25], with the obvious exception of defocus, which in our case is subjectively set. The results for the customized phase maps are shown in Fig. 11. For subject SM, word recognition acuity has a three-peak structure. Although the heights are not equal, the positions of the peaks are approximately correct if a shift in the best focus position is considered. For subject PA, the third peak is still missing but a slight increase at the tail of the curve can be seen. These results suggest that the interaction between the phase profile and the subject's aberration map is playing a role in this case.

4. Conclusions

The concept of Adaptive Optics Visual Simulation opens new lines of research in Physiological and Ophthalmic Optics. The manipulation of ocular aberrations and the possibility to explore their effects on different visual tasks can be of interest, e. g., for the study of higher level visual processes such as neural adaptation or for the design of new ophthalmic technologies. In this work we have proposed and demonstrated the capabilities of a Liquid Crystal Adaptive Optics Visual Simulator as a design tool for the development of ophthalmic optical elements with increased depth of focus. The active element of the system is a liquid crystal spatial light modulator, which has the advantages of high fidelity, allowing single step phase manipulation, and high spatial resolution, overcoming the continuity limitations of most deformable mirrors. The proposed apparatus allows the study of the stand-alone optical characteristics of a phase profile, the assessment of its impact on visual performance for different vergences, and the examination of its interaction with the eye's particular aberrations. This type of analysis can be used as a first step in the testing of a new model of ophthalmic optical element, constituting a kind of design loop. Results are shown for two different multifocal phase profiles obtained by a hybrid optimization method, which is described in the text. These two profiles were selected to exemplify two different possible outcomes of a visual simulation exam: one of them shows a behavior in good agreement with the design specifications while discrepancies appear for the other. The latter can be taken as an example of a model to be rejected or redesigned and, accordingly, the use of the LC-AOVS means a clear reduction of costs. Additionally, the data obtained could be used to improve the designs. Conversely, the former phase profile can be taken as a good candidate to be implemented in prototypes. In that case, since the behavior of the profile has been verified, the potential discrepancies that could be observed in further trials should be attributed to other factors, e.g., the prototype construction procedure, rather to failures in the design. Furthermore, the system can be used to perform visual testing through the said prototypes as a cross-checking. In conclusion, the LC-AOVS is a powerful tool for the design of new ophthalmic optical elements, reducing costs, saving steps, and eventually leading to better solutions.

Acknowledgements

This work has been supported in part by the Spanish Ministerio de Educación y Ciencia (grants FIS2004-2153, FIS2007-64765, CIT-020500-2005-031 and CIT-020400-2007-64).

#87831 - $15.00 USD Received 24 Sep 2007; revised 15 Nov 2007; accepted 19 Nov 2007; published 21 Nov 2007